Journal of Physics: Conference Series **438** (2013) 012009 doi:10.1088/1742-6596/438/1/012009

# New applications of the jellium model for the study of atomic clusters

**R G Polozkov[1], V K Ivanov[1], A V Verkhovtsev[1,2], A V Korol[2,3] and A V Solov'yov[2,4]**

[1] St. Petersburg State Polytechnic University, Politekhnicheskaya ul. 29, 195251 St. Petersburg, Russia
[2] Frankfurt Institute for Advanced Studies, Ruth-Moufang-Str. 1, 60438 Frankfurt am Main, Germany
[3] Department of Physics, St. Petersburg State Maritime Technical University, Leninskii prospekt 101, 198262 St. Petersburg, Russia

E-mail: verkhovtsev@fias.uni-frankfurt.de

**Abstract.** Application of the jellium model for investigation of the electronic structure and photoionization of metal clusters and fullerenes is discussed. The valence electrons are considered either within the Hartree-Fock and the local density approximations. The random phase approximation is utilized to account for the many-electron correlations in the response of a system to an external field. It is shown that the photodetachment cross section and photoelectron angular distribution in metal cluster anions are described reasonably well within the jellium model. Its application to fullerenes requires the use of corrections for a better description of the ground state electron density.

## 1. Introduction

Electronic structure, as well as photoexcitation and photoionization processes, of clusters have been studied for more than several decades. During this period a number of important achievements have been made. For instance, the geometrical structure of mass-selected clusters has been studied in detail experimentally by means of the low-temperature photoelectron spectroscopy and theoretically by using the density functional theory (DFT).

Among various types of atomic clusters, metal and carbon clusters have been of the main interest for studying (see, e.g., the reviews [1–4] and references therein). For instance, the geometrical structures of sodium cluster anions consisting of up to 350 atoms were determined with high accuracy by comparing results of the DFT calculations with measured photoelectron spectra [5–7]. It was shown that valence electrons form highly discretized density of states, the so-called electronic shell structure. Another achievement is associated with observation of the plasmon resonances in photoabsorption spectra of various small metal clusters, e.g., Na, K and Mg clusters (see [1, 2, 8] and references therein). It was established that in many cases the pattern structure of plasmon resonances is determined by the deformation parameter of a cluster as well as by the interaction between single-electron and collective excitation modes.

[4] On leave from A.F. Ioffe Physical-Technical Institute, St. Petersburg, Russia

Similar achievements have been made for fullerenes. For instance, it was shown that plasmon excitations can be formed in the processes of photon- or electron impact ionization of fullerenes. Having a profound collective nature, the plasmon excitations influence significantly the formation of broad resonance structures, the so-called giant resonances, in the the cross sections of different excitation processes. The plasmon excitations in the $C_{60}$ molecule have been intensively investigated both experimentally and theoretically (see, e.g. [9–17]). It was found that the photoionization cross section for the neutral fullerene $C_{60}$ possesses a very strong giant resonance centered at the photon energy about 20 eV [15]. Later on, a second collective excitation in $C_{60}$ and its ions, centered around the photon energy of 40 eV, was observed and discussed [17–20].

Recently, the photoabsorption spectrum of the $C_{60}$ fullerene was calculated in a broad photon energy range by means *ab initio* methods based on the time-dependent density functional theory [21, 22]. A detailed analysis of the calculated spectrum revealed the the contributions, coming out from single-particle and collective electron excitations [22].

At present, essential progress in experimental study of photoabsorption processes of clusters has been achieved by using new sources for free neutral [23] and charged [24] size-selected metal clusters. These measurements were followed by new theoretical calculations of the photoionization cross section [25–27] and of the photoelectron angular distribution for neutral and charged metal clusters [28, 29].

From the theoretical point of view, the valence electron-shell structure and optical properties of various atomic clusters were successfully described by means of the jellium model [30, 31]. Within the jellium model a cluster is considered as a object consisting of two systems: a system of valence electrons and an ionic core. The basic idea of the jellium model is to replace the real geometry of the ionic core by a smooth positive background in a finite volume and to treat only delocalized electrons explicitly in the mean-field approximation. The electron system is considered in a single-particle approach which can be the Hartree-Fock or the local density approximations. Since the collective many-electron effects play sometimes a crucial role in ionization processes of clusters, the dynamical many-electron correlations are usually also taken into account within the random phase approximation [32].

This article is devoted to some achievements of the recent applications of jellium model to metal clusters and fullerenes.

The atomic system of units, $m_e = |e| = \hbar = 1$, is used throughout the paper.

## 2. Application of the jellium model to clusters

The characteristic features of small metal clusters, like the electronic shell structure and plasmon excitations, can be well understood in terms of quantum motion of the delocalized valence electrons moving in the field created by themselves and by the positively charged ionic core [31]. This concept, known as the jellium model for neutral metal clusters, can also be applied to the charged systems.

In this section we consider so-called magic sodium clusters, namely $Na_{19}^-$ and $Na_{57}^-$, which can be treated as spherically symmetric objects due to the completely filled electronic shells. Within the jellium model the complicated ionic structure of the cluster can be reduced to the uniform spherically symmetric positive charge distribution. The potential $U_{\rm core}(r)$ generated by this distribution is equal to

$$U_{\rm core}(r) = \begin{cases} -\dfrac{Z}{2R_0}\left(3 - \left(\dfrac{r}{R_0}\right)^2\right) & , \; r \le R_0 \\ -\dfrac{Z}{r} & , \; r > R_0 \end{cases} , \qquad (1)$$

where $Z$ is the charge of the ionic core. For a neutral sodium cluster, $Z$ equals to the number of delocalized valence electrons $N$, coinciding with the number of atoms for clusters of monovalent elements. Therefore, for the singly charged anions the relation $Z = N - 1$ is fulfilled. The core radius $R_0$ is related to the charge as $R_0 = r_s Z^{1/3}$, where the Wigner-Seitz radius $r_s$ stands for the average distance between atoms in the bulk material. For the bulk sodium $r_s = 4$ a.u.

In a spherically symmetric field, a single-electron wave function is written as a product of radial, angular and spin wave functions:

$$\varphi_{nlm\sigma} = \frac{1}{r} P_{nl}(r) Y_{lm}(\theta, \phi) X_\sigma \ , \tag{2}$$

where $n$, $l$, $m$ and $\sigma$ are the principal, orbital, magnetic and spin quantum numbers, respectively. Solving self-consistently the system of $N$ single-particle equations (where $N$ is the number of delocalized electrons in a system), one obtains the single-electron wave functions $\varphi_i$ ($i \equiv nlm\sigma$) and the corresponding energies $\varepsilon_i$. The system of equations is usually solved within the Hartree-Fock (HF) or the local density (LDA) approximations.

The electronic shell structure of neutral and charged metal clusters corresponds to that in a short-range spherical potential. When the spin-orbit interaction is neglected, the shell with quantum numbers $\{n, l\}$ accommodates $2(2l + 1)$ electrons. Thus, the ground state electronic configurations of $Na_{19}^-$ and $Na_{57}^-$ clusters are defined as:

$$1s^2 2p^6 3d^{10} 2s^2 \text{ for } Na_{19}^- \ , \qquad 1s^2 2p^6 3d^{10} 2s^2 4f^{14} 3p^6 5g^{18} \text{ for } Na_{57}^-.$$

In the present study, the wave functions of a photoelectron are obtained from the HF equations as the solution corresponding to the energy $\varepsilon = \omega - I_p$ and satisfying certain asymptotic behavior (see, e.g. [32]), where $I_p$ is the ionization potential and $\omega$ is the photon energy. The wave functions of the excited states are calculated either in the field of the "frozen" core with the created vacancy or in the field of the rearranged residual electron structure of the cluster. The latter approximation is termed as the static rearrangement. The obtained HF radial wave functions $P_{nl}(r)$ and $P_{\varepsilon l}(r)$ are used further to calculate the dipole-photon amplitudes as well as the Coulomb matrix elements to account for many-electron correlations.

Below we discuss in more detail the photodetachment process from metal cluster anions. In recent works [5–7] the first measurements of the angular resolved photoelectron spectra of negatively charged sodium clusters were reported. The experiments were performed in a broad range of cluster sizes, $3 \leq Z \leq 147$, and allowed one to probe the angular momenta of single-electron orbitals. It was also demonstrated [7] that simple models based on single-electron treatment of the photoionization process fail to describe the angular anisotropy of photoelectrons. The first calculations performed within the framework of the jellium model for the ionic core and the random phase approximation with exchange (RPAE) for the valence electrons demonstrated a crucial role of many-electron correlations in describing the correct behavior of the photoelectron angular distribution [29]. The essential contribution of many-electron correlations in the photoionization process is not a surprise for neutral metal clusters. The correlations become even more pronounced for negative ions because of weaker binding of the valence electrons. As a result, the role of the continuous spectrum of excitations becomes even more important in the description of photoionization of negative ions, which is very interesting from the theoretical point of view.

The partial photodetachment cross section $\sigma_{nl}(\omega)$ of the $nl$ shell is given by the expression:

$$\sigma_{nl}(\omega) = \frac{4\pi^2 \alpha N_{nl}}{3(2l+1)\omega} \left( |d_{l+1}|^2 + |d_{l-1}|^2 \right) \ , \tag{3}$$

where $\alpha$ is the fine-structure constant, $\omega$ is the photon energy, $N_{nl}$ is the number of electrons in the $nl$ shell. The reduced HF dipole matrix elements $d_{l\pm1}$ (in the length form) are defined as follows:

$$d_{l\pm1} \equiv \langle \varepsilon l \pm 1 |\, d \,|\, nl \rangle = (-1)^l \sqrt{l_>} \int_0^\infty P_{nl}(r) P_{\varepsilon l\pm1}(r)\, r\, dr \ , \tag{4}$$

where $l_> = l + 1$ for the $l \to l + 1$ transition and $l_> = l$ for the $l \to l - 1$ transition. The total photodetachment cross section is obtained by the sum over all partial cross sections.

To account for many-electron correlations we use the RPAE scheme which describes the dynamic collective response of an electron system to an external electromagnetic field [32]. Within the RPAE, the dipole-photon amplitudes $\langle \varepsilon l \pm 1 |\, D(\omega) \,|\, nl \rangle$ are obtained by solving the following integral equation:

$$\langle \varepsilon l \pm 1 |\, D(\omega) \,|\, nl \rangle = \langle \varepsilon l \pm 1 |\, d \,|\, nl \rangle + \left( \sum_{\substack{\nu_2 > F \\ \nu_1 \le F}} - \sum_{\substack{\nu_1 > F \\ \nu_2 \le F}} \right) \frac{\langle \nu_2 |\, D(\omega) \,|\, \nu_1 \rangle \langle \nu_1, \varepsilon l \pm 1 |\, U \,|\, \nu_2, nl \rangle}{\omega - \varepsilon_2 + \varepsilon_1 + \imath\delta} \ . \tag{5}$$

Here the indices $\nu_1$ and $\nu_2$ denote the quantum numbers $\{n(\varepsilon), l\}$ of the virtual electron-hole states, $F$ is the Fermi energy, and the matrix element $\langle \dots |\, U \,| \dots \rangle$ stands for the sum of the direct and exchange Coulomb matrix elements [32].

The angular distribution of photoelectrons detached from the $nl$ shell by an unpolarized photon is determined by the differential cross section of the electron emission into the solid angle $d\Omega = \sin\theta d\theta d\phi$ [33]:

$$\frac{\mathrm{d}\sigma_{\mathrm{nl}}(\omega)}{\mathrm{d}\Omega} = \frac{\sigma_{nl}(\omega)}{4\pi} \left[ 1 - \frac{1}{2} \beta_{nl}(\varepsilon) P_2(\cos\theta) \right] \ , \tag{6}$$

where $P_2(\cos\theta)$ is the Legendre polynomial, $\beta_{nl}(\varepsilon)$ is the angular distribution anisotropy parameter, and $\varepsilon$ is the photoelectron energy.

The main feature of the total photoabsorption cross section in metal clusters is the giant plasmon resonance at about 2-3 eV which appears due to the collective response of the systems [8]. For neutral and positively charged clusters plasmon resonance lies in the discrete spectrum of electronic excitations. The simple HF scheme produces the set of single-electron excitations below the ionization potential and the corresponding distribution of the oscillator strengths. When the correlations are accounted for, the most of the oscillator strength becomes concentrated at the energy close to 2-3 eV, thus describing properly the plasmon excitation.

The distinguishing feature of negatively charged clusters is that they either do not have at all or have just 1-2 discrete dipole excitations. Therefore, the main part of the oscillator strength of partial transitions is distributed in the continuous spectrum of photodetachment cross section. This feature manifests itself both within the HF approximation and the RPAE. Thus, the plasmon resonance lies in continuum, and the account for many-electron correlations leads to significant change in the resonance position, its maximum value and the shape of the resonance curve [27].

The typical photodetachment cross section behavior for metal cluster anions, namely $Na_{19}^-$ and $Na_{57}^-$, is shown in figure 1 and reveals the powerful maxima due to the collective electron excitation. For the $Na_{19}^-$ anion (left panel), six dipole transitions were taken into account in the RPAE calculations. The dipole transitions from the outer $3d$ and $2s$ shells give the main contribution to the total cross section in the vicinity of the plasmon resonance which is located at about $\omega = 2.4$ eV. However, it should be noted that it is not enough to account only for the transitions from the outer shells in order to obtain the final profile of the plasmon excitation. Instead, one should include the interactions between all valence electrons.

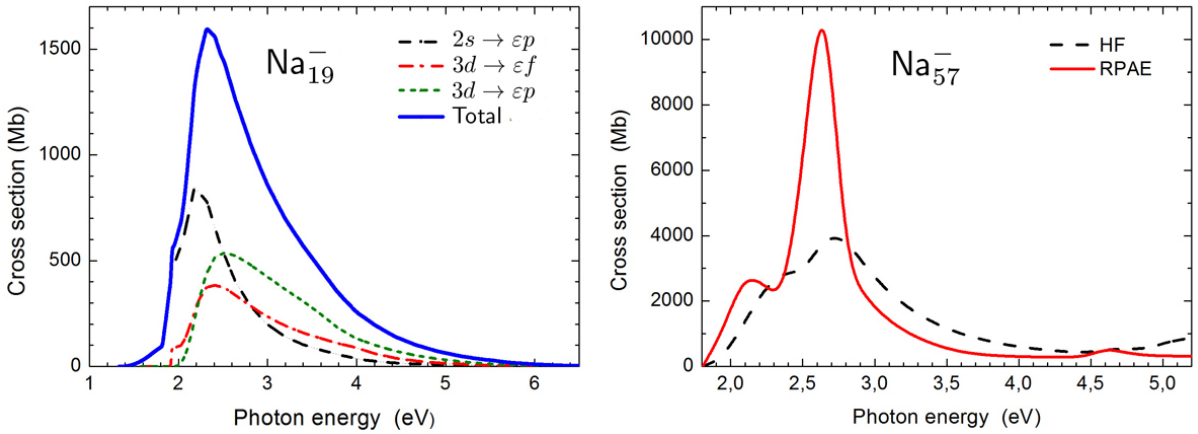


**Figure 1.** Left panel: the RPAE partial (dashed and dash-dotted lines) and total (solid line) photodetachment cross sections for the $Na_{19}^-$ anion. Right panel: the total cross section for $Na_{57}^-$ within the HF (dashed line) and RPAE (solid line).

For larger cluster anions the number of transitions, which must be accounted for, increases significantly. The total photodetachment cross sections of $Na_{57}^-$ calculated within the HF approximation and the RPAE are shown in the right panel of figure 1. The main contribution to the total cross section comes from the outer $5g$ shell. However, similar to the case of the $Na_{19}^-$ anion, to form the powerful resonance in the total cross section it is essential to take into account the contributions of several shells, namely of the $2s$, $3d$ and $3p$ shells. For $Na_{57}^-$ the position of the plasmon resonance is about $2.6 - 2.7$ eV, and, thus, it does not change significantly with the size of the cluster and lies very close to the classical Mie value.

It should be noted that the total photodetachment cross section is not a very sensitive indicator of the applicability of the jellium model to metal clusters. The photoelectron angular distribution represents a much better test for the conventional jellium model, since the behavior of the anisotropy parameter $\beta(\varepsilon)$ can show whether the shell structure is real and the orbital momentum $l$ is a good quantum number in the cluster system.

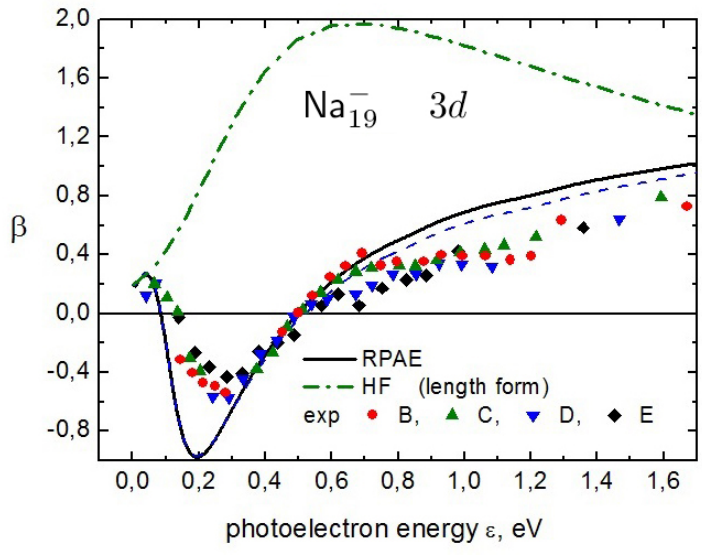


**Figure 2.** The angular anisotropy parameter $\beta(\varepsilon)$ for the $3d$ shell of the $Na_{19}^-$ anion as a function of photoelectron energy. Comparison between the HF (dash-dotted line), RPAE (solid line) and the experiment [6] (symbols). Experimental data marked as B, C, D and E correspond to the photoionization from the sublevels of the $3d$ orbital split by the crystalline field.

The comparison between the HF, the RPAE and the experimental data [6] for the outer $3d$ shell in the $Na_{19}^-$ anion is presented in figure 2. The experimental points marked as B, C, D and E correspond to the photoionization from the sublevels of the $3d$ orbital which is split by the crystalline field of the cluster in the range $1.75 - 2.15$ eV. It is interesting to note that the general behavior of photoelectron angular distribution is approximately the same for all sublevels. This indicates that all electrons in the sublevels can be characterized by the same orbital quantum number $l$. The $3d$ binding energy, which is equal to $I_{1d} = 1.92$ eV within the HF approximation, is very close to the center of the multiplet. The calculations within the HF framework (dash-dotted line) fail to explain the dependence of the angular anisotropy parameter on the photoelectron energy. On the contrary, the RPAE results (solid line) are in a good agreement with the experimental data. However, the HF and RPAE schemes based on the jellium model ignore the splitting and, thus, provide the average dependence of the angular anisotropy parameter.

As for larger clusters, we performed the calculations of the angular anisotropy parameter $\beta(\varepsilon)$ for several outer shells of the $Na_{57}^-$ anion. The experimental measurements of the photoelectron spectra were performed not for the closed-shell $Na_{57}^-$ anion, but for $Na_{55}^-$, which has the unfilled $5g^{16}$ shell [6, 7]. Note that despite of different cluster anions, considered theoretically and experimentally, as well as of the differences in ionization potentials, the general behavior of the angular anisotropy parameter for inner shells (for instance, for $4f$ shell, see the left panel of figure 3) is reproduced quite well by the performed many-body calculations.

However, for the outer $5g$ shell we can only state a qualitative agreement between the calculated results for $Na_{57}^-$ and the experimental data for $Na_{55}^-$ (the right panel of figure 3). Several reasons can be indicated which may explain the quantitative deviation. First, in our calculations we neglected the polarization potential which is rather large for neutral metal clusters and, thus, modifies the dynamics of the outgoing photoelectron. Second, the electrons in the open $5g^{16}$ shell in $Na_{55}^-$ are much stronger influenced by the crystalline field than the electrons in the filled $5g^{18}$ shell of $Na_{57}^-$.

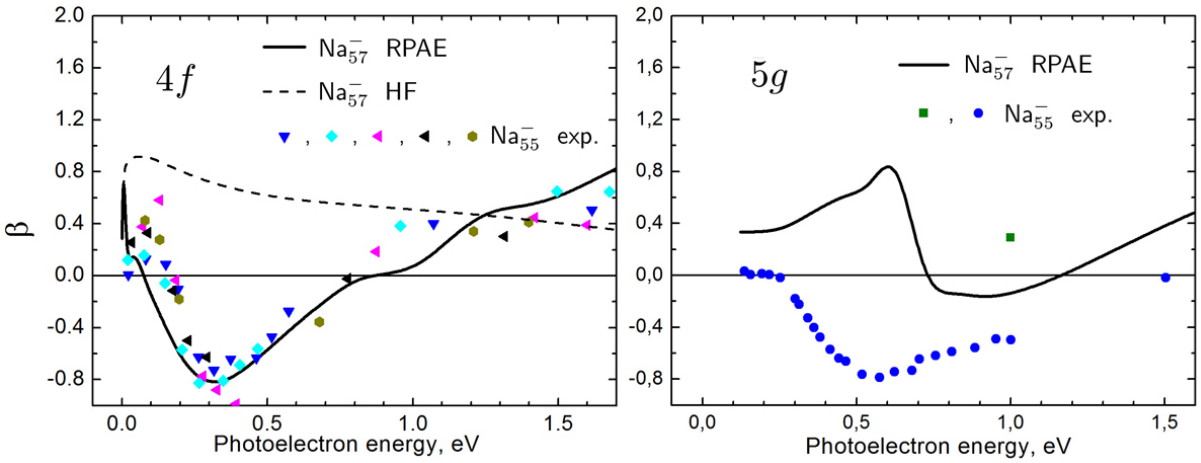


**Figure 3.** The angular anisotropy parameter for the $4f$ and $5g$ shells of $Na_{57}^-$ anion as a function of the photoelectron energy. Comparison between the HF (dashed line), the RPAE (solid line) results and the experiment data (symbols) in $Na_{55}^-$ taken from [6]. Different experimental points correspond to the photoionization from the sublevels of the orbital split by the crystalline field of the cluster.

The comparison of the existing experimental and theoretical data indicates that further investigation of the process is needed. The theoretical consideration of many-electron system

was performed using the simple jellium model for the ionic core. Of course, a more detailed analysis of the problem should go beyond this model and account for the realistic geometrical structure of the core. However, the agreement between the experimental data on the angular distribution and the results of the current theory indicates that the definite shell structure of valence electrons is reproduced quite well even neglecting the interaction with real crystalline field.

## 3. Application of the jellium model to fullerenes

*Ab initio* quantum-chemical calculations may provide an accurate quantitative description of the ground state of many-particle systems (atomic clusters and fullerenes, in particular) and allow one to obtain detailed information on geometrical and chemical properties of the system. Meanwhile, the description of dynamic properties, which play an important role in the processes of photoabsorption, elastic and inelastic scattering, electron attachment and photon emission, is a challenging task for the most of contemporary computer packages for *ab initio* based calculations. Dynamic properties (for example, dynamic polarizability) are closely related to the response of a many-electron system to an external electromagnetic field. In case of metal cluster anions and, especially, fullerenes, the properties are governed by collective electron excitations and formation of the plasmon resonances in the continuum [8]. Only recently it became possible to calculate the photoabsorption spectrum of many-electron systems in a broad photon energy range by means of the *ab initio* approach. For instance, it was done for the $C_{60}$ molecule [21,22].

The description of the collective excitations in the continuous spectrum can be performed comparatively easy by means of simplified model approximations. The advantage of such approaches is that they allow one to overcome significant computational difficulties but at the same time take into account the essential features of the processes providing clear physical insight into the phenomena. During the last decades the jellium model have been applied frequently to the description of ground-state properties of fullerenes [34], as well as to the investigation of photoexcitation processes arising in these systems [12,35–38].

In this section we consider the widely investigated $C_{60}$ molecule as a case study. It is assumed that the valence $2s^2 2p^2$ electrons in each carbon atom form a cloud of delocalized electrons, while the inner-shell $1s^2$ electrons are treated as frozen and are not taken into consideration. Thus, within the jellium model the fullerene core of the 60 charged carbon ions, $C^{4+}$, is replaced by an uniform distribution of positive charge $Z = 240$ over a spherical layer of a finite thickness, $\Delta R = R_2 - R_1$. The thickness $\Delta R$ is chosen to be equal to 1.5 Å which corresponds to a typical diameter of a carbon atom [39] and refers to experimental data from [37]. The potential of the core may be written as

$$U_{\text{core}}(r) = \begin{cases} -\dfrac{3Z(R_2^2 - R_1^2)}{2(R_2^3 - R_1^3)} & , \ r < R_1 \\ -\dfrac{Z}{2\left(R_2^3 - R_1^3\right)}\left(3R_2^2 - r^2\left(1 + \dfrac{2R_1^3}{r^3}\right)\right) & , \ R_1 \le r \le R_2 \\ -\dfrac{Z}{r} & , \ r > R_2 \end{cases} , \tag{7}$$

where $R_1 = R - \Delta R/2$ and $R_2 = R + \Delta R/2$ with $R$ standing for a fullerene radius, $R = 3.54$ Å for $C_{60}$. Supposing $R_1 \to 0$, one approaches the metal cluster limit, and equation (7) transforms into (1).

Since it is commonly acknowledged [40] that $C_{60}$, as well as other fullerenes, is formed from fragments of planar graphite sheets, it is natural to match the $\sigma$- and $\pi$-orbitals of graphite to the nodeless and the single-node wavefunctions of a fullerene, respectively [41]. Carbon atoms within a graphite sheet are connected by $\sigma$-bonds, whereas different sheets are connected by $\pi$-bonds. In the fullerene, the nodeless $\sigma$-orbitals are localized at the radius of the ionic core

while the single-node $\pi$-orbitals are oriented perpendicularly to the fullerene surface. The ratio of $\sigma$- to $\pi$-orbitals in $C_{60}$ should be equal to 3 : 1 due to the $sp^2$-hybridization of carbon orbitals [42]. Thereby, the electronic configuration of the delocalized electrons in $C_{60}$ is written in the form [34]:

$$1s^2 2p^6 3d^{10} 4f^{14} 5g^{18} 6h^{22} 7i^{26} 8k^{30} 9l^{34} 10m^{18} 2s^2 3p^6 4d^{10} 5f^{14} 6g^{18} 7h^{10} \quad .$$

Radial wavefunctions of the $1s \dots 10m$ shells are nodeless, while the wavefunctions of the $2s \dots 7h$ shells have one radial node each.

In the present study, the electronic subsystem of $C_{60}$ is treated within the LDA approach. In this case, the single-electron wavefunctions $\varphi_{nlm\sigma}(r)$ (see equation (2)) and the corresponding energies $\varepsilon_{nl}$ are determined from a system of self-consistent Kohn-Sham equations.

It is known [43, 44] that the results obtained within the conventional jellium model for fullerenes, while being qualitatively useful, can sometimes lead to unphysical conclusions. For instance, they can lead to unreliable values for the total energy of the ground state [43]. To avoid this, a phenomenological square-well (SW) pseudopotential (see, e.g., [35–37]) has been commonly added to jellium potential (7):

$$U_{\rm core}(r) \to \begin{cases} U_{\rm core}(r) + U_{\rm SW} & , \ R_1 \le r \le R_2 \\ U_{\rm core}(r) & , \ \text{otherwise} \end{cases} \quad , \tag{8}$$

where $U_{\rm SW}$ is an adjustable parameter to correct the obtained electronic structure.

It was claimed that accounting for such a pseudopotential increases the accuracy of the jellium-based description and, for instance, allows one to reproduce the experimental value of the first ionization potential of $C_{60}$ [35]. Nonetheless, the applicability of the jellium model for fullerenes and the choice of parameters of the used SW pseudopotential have not been clearly justified so far from a physical viewpoint. Besides, this simple approach cannot describe properly the valence electron density distribution (see the solid red line in the left panel of figure 4) what is critical for the calculation of dynamical polarizability. In the recent work [45], the structured pseudopotential correction $\Delta U$, originated from the comparison of an accurate *ab initio* calculation with the jellium-based one, was proposed:

$$\Delta U(r) = \bar{U}^{\rm QC}_{\rm core}(r) - U^{\rm jel}_{\rm core}(r) \ , \tag{9}$$

where $\bar{U}^{\rm QC}_{\rm core}(r)$ is the potential of the fullerene core obtained from quantum-chemical calculations and averaged by spherical angles variables, and $U^{\rm jel}_{\rm core}(r)$ is the jellium core potential (7). It was shown [45] that such correction to the conventional jellium model allows one to account, at least partly, for the $sp^2$-hybridization of carbon atomic orbitals, and can predict the shape of the electron density in a more realistic way (see the dash-dotted blue line in the right panel of figure 4).

The photoionization process is studied in a way similar to that described in section 2 for the metal cluster anions. The partial photoionization cross section $\sigma_{nl}(\omega)$ of the $nl$-shell of a fullerene is defined by equation (3). Using the single-electron wavefunctions (here we used the LDA approach) one can calculate the one-particle transition amplitudes $d_{l\pm1}$. To take into account the collective electron excitations in fullerenes we solved equation (5). Describing the single-particle interaction within the LDA approach, one should then exclude the exchange interaction in the matrix elements $\langle \dots | U | \dots \rangle$, replacing the latter by the ordinary direct Coulomb matrix element in equation (5). Thus, one obtains the reduced amplitudes $D_{l\pm1}(\omega)$, which include the many-electron correlations within the random phase approximation (RPA).

Using the correction introduced, one improves the description of the ground state density distribution within the jellium model and obtains a more realistic electron density as compared to the conventional model. Using the corrected jellium potential, we calculated in the present

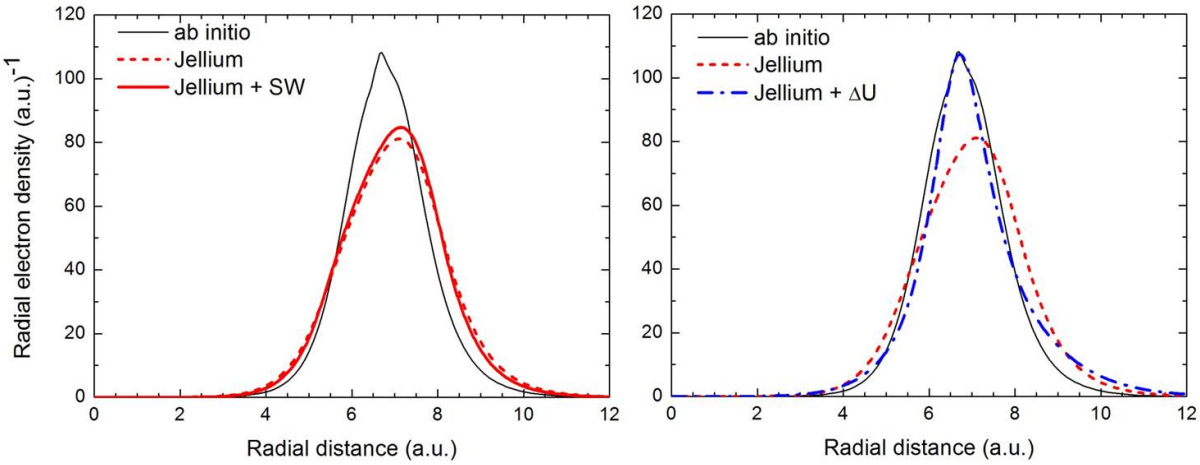


**Figure 4.** Radial electron density of $C_{60}$ obtained from the *ab initio* calculation (solid black line) and calculated by means of the jellium model: the conventional one (dashed red curve), with the additional square well (SW) pseudopotential (solid red curve) and with the correction $\Delta U$ (dash-dotted blue curve).

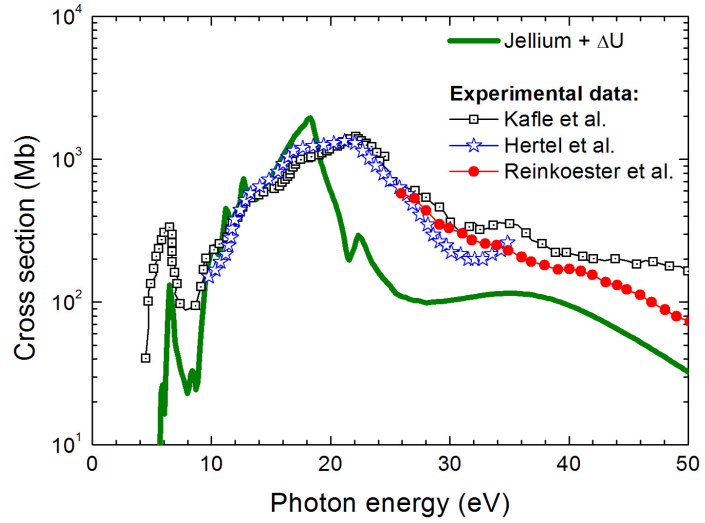


**Figure 5.** Photoionization cross section of $C_{60}$ obtained from LDA calculations within jellium model with structured correction $\Delta U$ (solid green line) and comparison with available experimental data from Hertel *et al.* [15], Reinköster *et al.* [17] and Kafle *et al.* [16]. Many-electron correlations were accounted for in the calculations within the RPA approach.

study the total photoionization cross section of $C_{60}$ within the LDA and RPA approaches. Results of the calculations and the comparison with experimental data [15–17] are presented in figure 5. It is seen that the calculated cross section can describe qualitatively main features of the spectrum in spite of some quantitative discrepancies. It should be noted that the cross section calculated using the corrected jellium model gives a better agreement with experimental data as compared to previous calculations performed within the conventional jellium model (see, e.g. [11, 12]).

## 4. Conclusion

In this paper we discussed the new applications of the jellium model for the study of photoexcitation processes in various atomic clusters. The consistent many-body theory was

applied to calculate the photodetachment cross sections of metal cluster anions as well as the angular distributions of photoelectrons. The case study analysis was performed for sodium cluster anions $Na_{19}^-$ and $Na_{57}^-$ which possess nearly spherical geometry due to the closure of electronic shells of delocalized electrons. The calculations revealed an important role of many-electron correlations in the formation of the giant plasmon resonance and in the angular distributions of photoelectrons, and allowed us to explain the behavior of the angular anisotropy parameter $\beta(\varepsilon)$ versus photoelectron energy in the recent experiments with sodium clusters [6,7].

The theoretical consideration of many-electron system was performed using the jellium model for the ionic core. Of course, a more detailed analysis of the problem should go beyond this model and account for the realistic geometrical structure of the core. However, the agreement between the experimental data on the angular distribution and the results of the current theory indicates that the definite shell structure of valence electrons is reproduced quite well even neglecting the interaction with a real crystalline field.

We discussed also a new type of correction for the description of fullerenes within the spherically symmetric jellium model. The correction represents an additional pseudopotential which originates from the difference between the precise *ab initio* calculation and the one within the jellium model. This potential allows one to mimic partially the $sp^2$-hybridization, which occurs in formation of fullerenes, and, thus, to import the hybridization effects into the conventional jellium model. It was shown that the correction used improves significantly the electron density distribution as compared to the standard jellium model and the one with an additional square-well pseudopotential. Like the other previously used corrections, it does not allow one to obtain a quantitative agreement with an *ab initio* calculation for the single-electron energy spectrum but reproduces the sequence of energy levels corresponding to the one following from the more precise quantum-chemical calculation [45]. Using this correction to the jellium model we calculated the dynamic response of fullerenes in the photoionization process. We showed that improving the description of the fullerene ground state, one can get a reasonable qualitative agreement with the experimentally measured photoionization cross sections [15–17].

## Acknowledgments

R.G.P. and V.K.I. thank the Frankfurt Institute for Advanced Studies for financial support and hospitality.

## References

[1] Brack M 1993 *Rev. Mod. Phys.* **65** 677
[2] de Heer W A 1993 *Rev. Mod. Phys.* **65** 611
[3] Connerade J-P and Solov'yov A V 2004 *Latest Advances in Atomic Clusters Collisions: Fission, Fusion, Electron, Ion and Photon Impact* (London: Imperial College Press)
[4] Connerade J-P and Solov'yov A V 2008 *Latest Advances in Atomic Clusters Collisions: Structure and Dynamics from the Nuclear to the Biological Scale* (London: Imperial College Press)
[5] Kostko O, Huber B, Moseler M and von Issendorff B 2007 *Phys. Rev. Lett.* **98** 043401
[6] Bartels C, Hock C, Huwer J, Kuhnen R, Schwöbel J and von Issendorff B 2009 *Science* **323** 1323
[7] Bartels C 2008 PhD thesis (Faculty of Mathematics and Physics, University of Freiburg)
[8] Solov'yov A V 2005 *Int. J. Mod. Phys.* B **19** 4143
[9] Bertsch G F, Bulgac A, Tomanek D and Wang Y 1991 *Phys. Rev. Lett.* **67** 2690
[10] Alasia F, Broglia R A, Roman H E, Serra L, Colo G and Pacheco G M 1994 *J. Phys. B: At. Mol. Opt. Phys.* **27** L643
[11] Ivanov V K, Kashenock G Yu, Polozkov R G and Solov'yov A V 2001 *J. Phys. B: At. Mol. Opt. Phys.* **34** L669
[12] Polozkov R G, Ivanov V K and Solov'yov A V 2005 *J. Phys. B: At. Mol. Opt. Phys.* **38** 4341
[13] Verkhovtsev A V, Korol A V, Solov'yov A V, Bolognesi P, Ruocco A and Avaldi L 2012 *J. Phys. B: At. Mol. Opt. Phys.* **45** 141002
[14] Bolognesi P, Ruocco A, Avaldi L, Verkhovtsev A V, Korol A V and Solov'yov A V 2012 *Eur. Phys. J.* D **66** 254

[15] Hertel I V, Steger H, de Vries J, Weisser B, Menzel C, Kamke B and Kamke W 1992 *Phys. Rev. Lett.* **68** 784
[16] Kafle B P, Katayanagi H, Prodhan M, Yagi H, Huang C and Mitsuke K 2008 *J. Phys. Soc. Jpn.* **77** 014302
[17] Reinköster A, Korica S, Prümper G, Viefhaus J, Godehusen K, Schwarzkopf O, Mast M and Becker U 2004 *J. Phys. B: At. Mol. Opt. Phys.* **37** 2135
[18] Scully S W J *et al* 2005 *Phys. Rev. Lett.* **94** 065503
[19] Korol A V and Solov'yov A V 2007 *Phys. Rev. Lett.* **98** 179601
[20] Scully S W J *et al* 2007 *Phys. Rev. Lett.* **98** 179602
[21] Chen Z and Msezane A Z 2012 *Phys. Rev.* A **86** 063405
[22] Verkhovtsev A V, Korol A V and Solov'yov A V 2013 (submitted)
[23] Huttula M, Mikkelä M-H, Tchaplyguine M and Bjorneholm O 2010 *J. Electron Spectrosc. Relat. Phenom.* **181** 145
[24] von Issendorff B and Cheshnovsky O 2005 *Annu. Rev. Phys. Chem.* **56** 549
[25] Jänkälä K, Mikkelä M-H and Huttula M 2011 *J. Phys. B: At. Mol. Opt. Phys.* **44** 105101
[26] Jänkälä K, Tchaplyguine M, Mikkelä M-H, Bjorneholm O and Huttula M 2011 *Phys. Rev. Lett.* **101** 183401
[27] Polozkov R G, Ivanov V K, Korol A V and Solov'yov A V 2012 *Eur. Phys. J.* D **66** 287
[28] Wopperer P, Faber B, Dinh P M, Reinhard P-G and Suraud E 2010 *Phys. Rev.* A **82** 063416
[29] Solov'yov A V, Polozkov R G and Ivanov V K 2010 *Phys. Rev.* A **81** 021202(R)
[30] Knight W D, Clemenger K, de Heer W A, Saunders W A, Chou M Y and Cohen M L 1984 *Phys. Rev. Lett.* **52** 2141
[31] Ekardt W 1999 *Metal clusters* (New York: John Wiley)
[32] Amusia M Ya 1990 *Atomic Photoeffect* (New York-London: Plenum Press)
[33] Cooper J and Zare R N 1968 *J. Chem. Phys.* **48** 942
Cooper J and Zare R N 1968 *J. Chem. Phys.* **49** 4252
[34] Yabana K and Bertsch G F 1993 *Phys. Scr.* **48** 633
[35] Puska M J and Nieminen R M 1993 *Phys. Rev.* A **47** 1181
Puska M J and Nieminen R M 1994 *Phys. Rev.* A **49** 629 (erratum)
[36] Wendin G and Wästberg B 1993 *Phys. Rev.* B **48** 14764
[37] Rüdel A, Hentges R, Becker U, Chakraborty H S, Madjet M E and Rost J-M 2002 *Phys. Rev. Lett.* **89** 125503
[38] Belyaev A K, Tiukanov A S, Toropkin A I, Ivanov V K, Polozkov R G and Solov'yov A V 2009 *Phys. Scr.* **80** 048121
[39] Östling D, Apell P and Rosen A 1993 *Europhys. Lett.* **21** 539
[40] Zhang Q L, O'Brien S C, Heath J R, Liu Y, Curl R F, Kroto H W and Smalley R E 1986 *J. Phys. Chem.* **90** 525
[41] Martins J L, Troullier N and Weaver J H 1991 *Chem. Phys. Lett.* **180** 457
[42] Haddon R C, Brus L E and Raghavachari K 1986 *Chem. Phys. Lett.* **125** 459
[43] Yannouleas C and Landman U 1994 *Chem. Phys. Lett.* **217** 175
[44] Pavlyukh Y and Berakdar J 2010 *Phys. Rev.* A **81** 042515
[45] Verkhovtsev A V, Polozkov R G, Ivanov V K, Korol A V and Solov'yov A V 2012 *J. Phys. B: At. Mol. Opt. Phys.* **45** 215101